



## ELECTRODEPOSITION OF NANO CRYSTALLINE ZINC FROM ACID BROMIDE BATH AND CHARACTERISATION

M. CHANDRAN\* and G. N. K. RAMESH BAPU<sup>a</sup>

Vivekananda College, Agasteeswaram, KANYAKUMARI – 629701 (T.N.) INDIA

<sup>a</sup>Central Electro Chemical Research Institute, KARAIKUDI – 630006 (T.N.) INDIA

(Received : 06.08.2013; Revised : 15.08.2013; Accepted : 17.08.2013)

### ABSTRACT

Zinc has been the widely used electrodeposits for protection against corrosion because of sacrificial action. Zinc bath to produce nano zinc coatings were optimised using Hull cell studies. Characterisations of the bath and deposits were performed. The surface morphology of the zinc deposits were studied by scanning electron microscopy (SEM). The preferred orientation and average size of the zinc electrodeposited particles were determined by X-ray diffraction analysis. The present studies showed that additives in the deposition process of zinc significantly increased the corrosion resistance.

**Key words:** Electrodeposition, Bromide bath, Nano crystalline zinc, Corrosion resistance.

### INTRODUCTION

Electrodeposited zinc coatings offer good corrosion resistance to steel substrates because of sacrificial action<sup>1</sup>. Different types of plating solutions like cyanide, acid and non-cyanide alkaline<sup>2-6</sup> are used for zinc electrodeposition. Recent trend on zinc plating is to develop plating solutions, which are eco friendly. The matte white nature of zinc deposits can be improved to bright using brighteners in the bath<sup>7-10</sup>. Bright deposits improve the appearance of the article, besides offering good corrosion resistance. Electrodeposition is a versatile materials processing technique finding applications ranging from miniature electronic devices to giant industrial structures as functional and/or aesthetic coatings. Both aqueous<sup>11</sup> and non aqueous<sup>12,13</sup> solutions have been employed for the purpose. However, the aqueous solutions have the special advantage of room temperature operation and are, therefore, preferred for large scale applications. Surface morphology, preferred orientation, and grain size, which are all influenced by processing conditions, have a significant effect on the mechanical properties of zinc electrodeposits. It is known that almost all mechanical properties can be effectively improved by refining the grain size, which is one reason nano crystalline materials have recently received considerable attention<sup>14</sup>. Accordingly, many efforts have been made by researchers in order to refine the grain size of zinc coatings and improve their properties<sup>15-17</sup>. The use of additives in electrodeposition solutions is extremely important due to their influence on the growth and structure of the resulting deposits. The presence of additives has been shown to influence physical and mechanical properties of electrodeposits such as grain size, brightness, internal stress; pitting and even chemical composition. Electrodeposition technique can yield porous-free finished products that do not require subsequent consolidation processing<sup>18</sup>.

In this present investigation, nano crystalline zinc coating was obtained from acid bromide bath. An attempt has been made to study the bath and deposit characteristics. The crystal structure of the electrodeposited nano crystalline zinc was investigated using SEM and XRD analyses. The corrosion resistance of nano crystalline zinc deposit was also studied.

## EXPERIMENTAL

All the solutions were prepared from AR grade chemicals (Loba Chemie) and double-distilled water. High purity (99.9%) zinc was used as the anode. The anode was activated each time by immersing in 10% HCl followed by water wash. Mild steel plates were mechanically polished to obtain a smooth surface and subjected to the usual pretreatments like solvent degreasing, alkaline electro cleaning and 5% acid dip. The optimum current density range for obtaining quality deposits from the basic bath was determined by Hull cell experiment using a standard 267 mL cell<sup>19</sup>. The thickness of the deposit on the Hull cell panel at different point was assessed by Elcometer 456 thickness gauge. The cathode current efficiency (CCE) and rate of build up at different current densities were determined from the weight of deposit on the cathode of (2.5 x 7.5) cm size.

Throwing power (TP) was measured in a Haring-Blum<sup>20</sup> cell. A porous zinc anode was placed between two parallel steel cathodes filling the rectangular cell cross section. One of the cathodes was nearer to anode than the other. The distance ratio was 5:1. The percentage of the throwing power was calculated from Field's formula<sup>21</sup>.

Micro hardness of electrodeposits of zinc was determined on the Vicker's scale by using LECO Tester. In this method, a diamond pyramid was pressed into the deposit under a load of 25 g for 15 seconds and the indentation diagonal was measured after the load was removed. The micro hardness of the deposit in Kg/mm<sup>2</sup> was determined in each case by using the formula.

$$\text{Vicker's Hardness (Kg/mm}^2\text{)} = \frac{1854 \times P}{d^2}$$

where p - The load applied in grams and

d - Diagonal of the indentation obtained in micrometers

The morphology of the electrodeposits was examined at x 5000 magnification to assess the grain size, deposit nature, heterogeneities and pores present in the deposits using a scanning electron microscope (JEOL-JSM-35 LF). X-ray diffraction (Philips TW 3710) was carried out using nickel-filtered Cu-K $\alpha$  radiation for determining the lattice parameter, crystallographic texture and approximate grain size of the deposit. The grain sizes of the coating were determined using the Scherrer's equation<sup>22</sup>.

The corrosion resistance of electrodeposited zinc was carried out in 3.5% NaCl by potentiodynamic polarization method, deposits obtained at an optimum current density of 2 A/dm<sup>2</sup>. Potentiodynamic polarization experiments were carried out using BioLogic SP-150 instruments. A large platinum foil (2.56 cm<sup>2</sup>) and saturated calomel electrode (SCE) were employed as auxiliary and reference electrodes, respectively.

## RESULTS AND DISCUSSION

### Cathode current efficiency and throwing power

Table 1 presents the bath compositions used in the present investigation. The influence of current

density on deposition characteristics of bath A and B under moderate agitation are given in Table 2. The results show that the cathode current efficiency increases with current density up to 2.0 A/dm<sup>2</sup> and then decreases with further increase in current density. This is due to the hydrogen evolution occurring at the cathode along with zinc deposition at the high current densities. The rate of build up increased with current density. Matte white deposits were obtained in the absence of additives, whereas in the presence of polyethylene glycol and glucose, semi bright and semi bright milky deposits were obtained.

The thickness of zinc deposits on the Hull cell plates at different points from high current density is given in Fig. 1. The variation of thickness with current density is an indication of throwing power.

Throwing power values at different current densities for bath A and bath B are given in Table 3. Throwing power of 10.27% was observed for the bath B at 2.0 A/dm<sup>2</sup> where as + 7.44% for the bath A at 2.0 A/dm<sup>2</sup>. Deposition from complex baths usually takes place at higher cathode potentials and hence it is associated with enhanced throwing power<sup>23</sup>. On the other hand non-complexing electrolytes are associated with less throwing power.

**Table 1: Bath compositions used in the present investigation**

Bath	Constituents	Composition (g/L)
A	Zinc bromide	160
	Boric acid	40
	Potassium bromide	40
	pH	4
B	Zinc bromide	160
	Boric acid	40
	Potassium bromide	40
	PEG	1.0
	Glucose	2.0
	pH	4

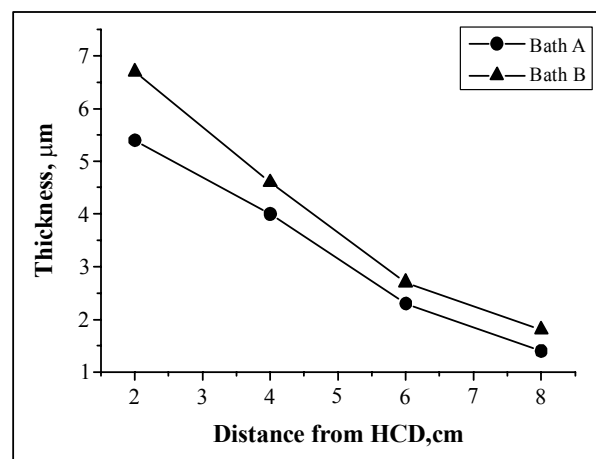


**Fig. 1: Variation of thickness of zinc deposits with current density on the Hull cell panel**

**Table 2: Effect of current density on deposition characteristics of baths A and B at 30°C under moderate agitation**

Bath	Current density (A/dm <sup>2</sup> )	Current efficiency (%)	Rate of build up (µm/hr)	Nature of the deposit
A	1.0	98.0	8.04	Matte white
	2.0	97.4	15.99	Matte white
	3.0	96.8	23.84	Matte white
	4.0	93.2	30.60	Matte white
B	1.0	92.6	7.60	Semi bright
	2.0	95.7	15.71	Semi bright
	3.0	94.5	23.27	Semi bright milky
	4.0	91.3	29.98	Semi bright milky

**Table 3: Throwing power for electrodeposition of zinc baths A and B at 30°C**

Bath	Current density (A/dm <sup>2</sup> )	Throwing power (%)
A	1.0	+ 6.12
	2.0	+ 8.04
B	1.0	+ 10.58
	2.0	+ 12.64

### Micro hardness

The results of micro hardness of zinc electrodeposits of 35 µm are given in Table 4. The hardness of 116 Kg/mm<sup>2</sup> was obtained for the zinc deposit from bath B and 65 Kg/mm<sup>2</sup> from bath A at 1.0 A/dm<sup>2</sup>. Hardness values obtained at 2 A/dm<sup>2</sup> showed a lesser value irrespective of the bath compared to values for 1 A/dm<sup>2</sup>. The deposits were found to be coarse at higher current density and hence a decreased value was obtained.

**Table 4: Micro hardness of electrodeposits from various baths A and B at 30°C**

Bath	Current density (A/dm <sup>2</sup> )	Vicker's micro hardness (Kg/mm <sup>2</sup> )
A	1.0	65
	2.0	58
B	1.0	116
	2.0	108

### Surface morphology of zinc deposits

The SEM micrographics showing structures of zinc deposits are given in Figs. 2 (a) and 2 (b). When viewed at 5000 X magnification in the scanning electron microscope, the zinc deposits 'A' exhibited non-uniform crystals growth with slightly large crystals. The surface of the zinc deposits 'B' exhibited a regular uniform arrangement of crystals, indicating a uniform throwing power and hence produced semi bright deposit.

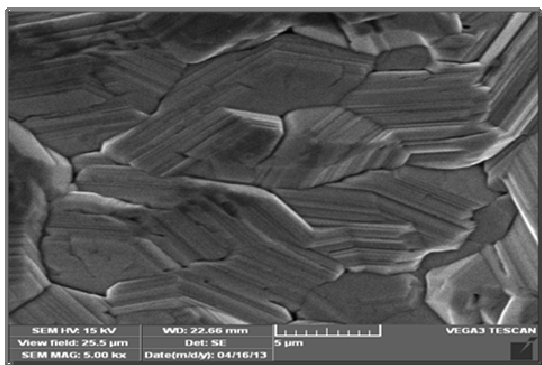


Fig. 2 (a): SEM photograph of deposit A

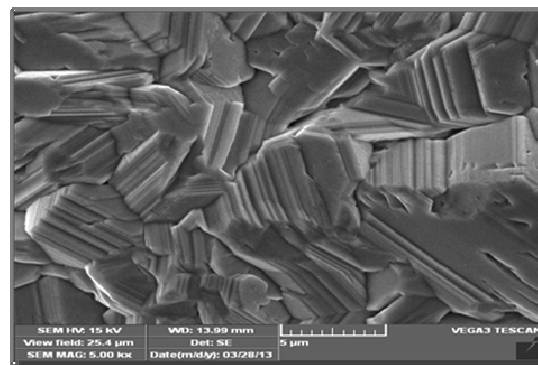


Fig. 2 (b): SEM photograph of deposit B

### Structure of zinc deposits

XRD patterns of zinc electrodeposits A and B are given in Figs. 3 (a) and 3 (b) and the corresponding XRD data in Tables 5 and 6, respectively. The observed 'd' value is in good agreement with the standard values for zinc deposition (Joint Committee on Powder Diffraction System/ASTM File No. 1\* 40831Zn). Crystalline size was determined from the full width at half maximum (FWHM) of the X-ray peaks using Scherrer's equation. The average crystal size of the deposit B was approximately 64 nm where as for deposit A was 142 nm.

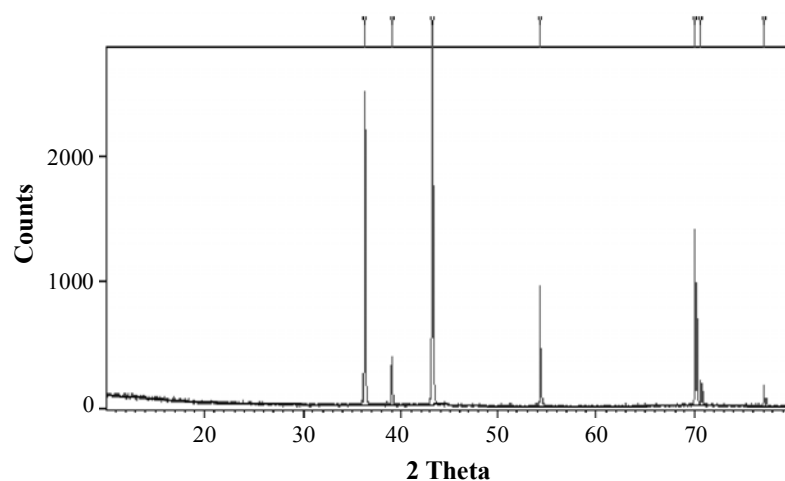
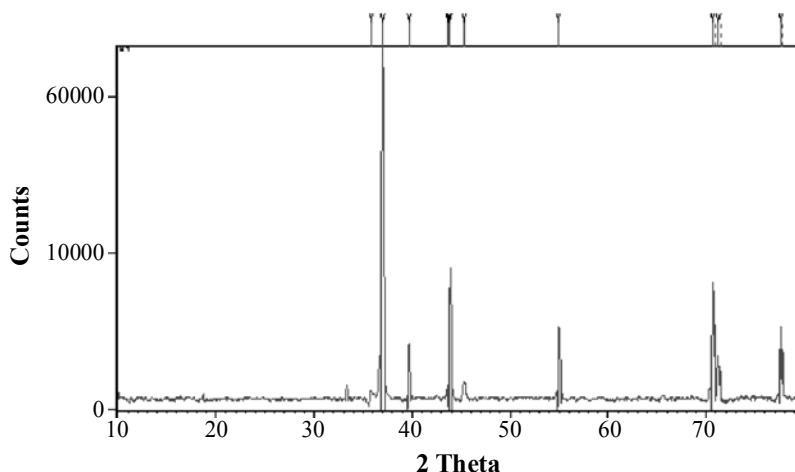


Fig. 3 (a): XRD patterns of zinc deposit A

Table 5: Parameters derived from XRD pattern for deposit A

S. No.	2θ (degree)	d (observed) (Å)	d (standard) (Å)	h k l	Average crystal size (nm)
1	36.29	2.475	2.473	0 0 2	166.99
2	39.00	2.308	2.308	1 0 0	126.32
3	43.23	2.092	2.091	1 0 1	170.69
4	54.33	1.687	1.687	1 0 2	146.29
5	70.65	1.332	1.332	1 1 0	119.66
6	77.04	1.236	1.236	0 0 4	124.78



**Fig. 3 (b): XRD patterns of zinc deposit B**

**Table 6: Parameters derived from XRD pattern for deposit B**

S. No.	2θ (degree)	d (observed) (Å)	d (standard) (Å)	h k l	Average crystal size (nm)
1	36.97	2.430	2.473	0 0 2	53.36
2	39.67	2.271	2.308	1 0 0	53.80
3	43.65	2.071	2.091	1 0 1	71.51
4	54.94	1.671	1.687	1 0 2	57.03
5	70.85	1.332	1.332	1 1 0	67.84
6	77.59	1.229	1.237	0 0 4	60.84

### Corrosion studies

From the electrochemical theory of corrosion, corrosion current densities can be obtained by extrapolating the linear segments of anodic and cathodic ( $E$ -log  $i$ ) curves. The slopes of the linear segments of anodic and cathodic branches give the anodic and cathodic Tafel slopes.

$$b_a = \text{Anodic Tafel slope} = RT/\alpha_a F$$

$$b_c = \text{Cathodic Tafel slope} = RT/-\alpha_c F$$

where  $\alpha_a$  and  $\alpha_c$  are transfer coefficients.

Figs. 4 (a) and 4 (b) present the polarization curves for zinc deposits A and B, respectively. Table 7 gives corrosion potential ( $E_{\text{corr}}$ ), corrosion current density ( $i_{\text{corr}}$ ), anodic and cathodic Tafel slopes during the polarization behaviour of the zinc samples in 3.5% sodium chloride solution. From the results, it can be seen that  $i_{\text{corr}}$  values for zinc deposits were considerably lowered in the presence of polyethylene glycol and glucose in the bath. The corrosion current densities for zinc deposit follow the order.

Deposit A > Deposit B

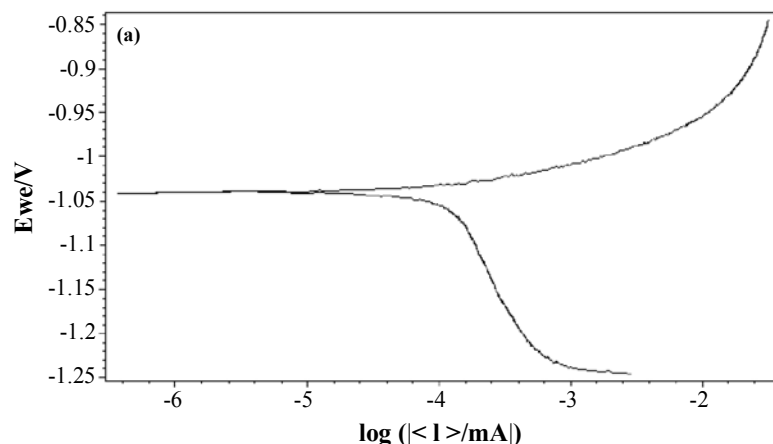


Fig. 4 (a): Polarization curve for zinc deposit A

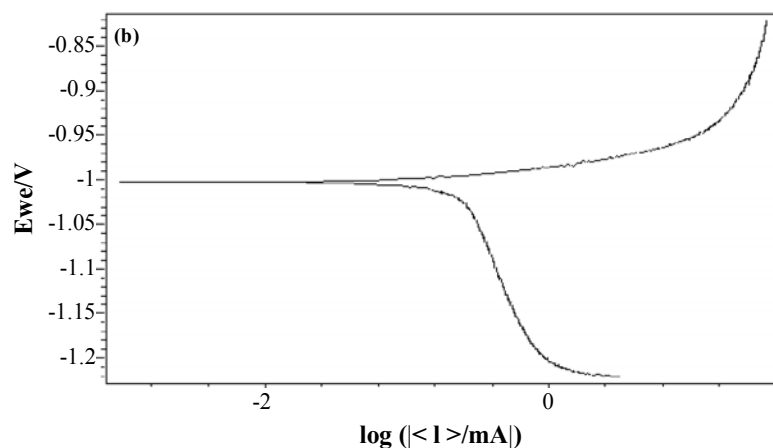


Fig. 4 (b): Polarization curve for zinc deposit B

Table 7: Parameters derived from E-log  $i$  curves for zinc deposits A and B in 3.5% sodium chloride solution at pH 7

Bath	Thickness ( $\mu\text{m}$ )	$E_{\text{corr}}$ (mV vs.SCE)	$i_{\text{corr}}$ ( $\mu\text{A}/\text{cm}^2$ )	Tafel slope (mV/decade)	
				$b_a$	$b_c$
A	16	-1042.143	94.486	251.9	33.3
B	16	-1029.578	44.255	239.9	10.7

## CONCLUSION

From the experiments carried out, polyethylene glycol and glucose in the zinc plating bath produced semi bright and semi bright milky, uniform and fine grained deposit with average crystalline size of 64 nm and the deposit exhibited better corrosion resistance.

## ACKNOWLEDGEMENT

The author (M. Chandran) expresses his sincere thanks to University Grants Commission, Government of India, New Delhi, for having the financial assistance under minor research project. He is also grateful to the Management, Vivekananda College, Agasteeswaram, Kanyakumari, for the encouragement given in his research pursuits.

**REFERENCES**

1. R. M. Krishnan, C. J. Kennedy, S. Jayakrishnan, S. Sriveeraraghavan and S. R. Natarajan, *Met. Finish.*, **94(10)**, 43 (1996).
2. R. Sekar, R. M. Krishnan, V. S. Muralidharan and S. Jayakrishnan, *Trans. Inst. Met. Finish.*, **83(2)**, 104 (2005).
3. K. Raeissi, M. A. Golozar, A. Saatchi and J. A. Szpunar, *Trans. Inst. Met. Finish.*, **83(2)**, 99 (2005).
4. A. Senthil Kumar, C. Senthilrajapandian, J. Ayyapparaju and G. N. K. Ramesh Babu, *Bull. Electrochem.*, **17(8)**, 379 (2001).
5. M. Chandran, R. L. Sarma and R. M. Krishnan, *Plat. Surf. Fin.*, **88(4)**, 74 (2001).
6. Shanmughasigamoni and M. Pushpavanam, *J. Appl. Electrochem.*, **36**, 315 (2006).
7. H. B. Muralidhara, Y. Arthoba Naik, H. P. Sachin and T. V. Venkatesha, *Indian J. Chem. Tech.*, **15**, 155 (2008).
8. R. Sekar, S. Sriveeraraghavan and R. M. Krishnan, *Bull. Electrochem.*, **15(5-6)**, 219 (1999).
9. P. Leisner and M. E. Benzon, *Trans. Inst. Met. Finish.*, **75(2)**, 88 (1997).
10. H. B. Muralidhara, Y. Arthoba Naik, H. P. Sachin, G. Achary and T. V. Venkatesh, *Indian J. Chem. Tech.*, **15**, 259 (2008).
11. J. Ahmad, K. Asami, A. Takeuchi, D. V. Louzguine and A. Inoue, *Mater. Trans.*, **44**, 911 (2003).
12. M. Mehmood, N. Kawaguchi, H. Maekawa, Y. Sato, T. Yamamura, M. Kawai, K. Kikuchi and M. Furusaka, *Mater. Trans.*, **44**, 1659 (2003).
13. M. Mehmood, N. Kawaguchi, H. Maekawa, Y. Sato, T. Yamamura, M. Kawai and K. Kikuchi, *Mater. Trans.*, **44**, 259 (2003).
14. H. Gleiter, *Progress in Materials Science*, **33**, 223 (1989).
15. K. O. Nayana, T. V. Venkatesha, B. M. Praveen and K. Vathsala, *J. Appl. Electrochem.*, **41**, 39 (2011).
16. H. B. Muralidhara and Y. Arthoba Naik, *Bull. Mater. Sci.*, **31(4)**, 585 (2008).
17. H. B. Muralidhara, Y. Arthoba Naik, T. V. Venkatesha, *Int. J. Chem. Sci.*, **10(1)**, 524 (2012).
18. H. B. Muralidhara, J. Balasubramanyam, Y. Arthoba Naik, K. Yogesh Kumar, H. Hanumanthappa, M. S. Veenaa, *J. Chem. Pharm. Res.*, **3(6)**, 433 (2011).
19. R. Gabe and G. D. Willcox, *Trans. Inst. Met. Finish.*, **71(2)**, 71 (1993).
20. H. Silmen, G. Isserlis and A. F. Averill (Ed.), *Preventive and Decorative Coatings for Metals*, Finishing Publications Ltd., Teddington, England (1978).
21. M. Mc Cormick and A. T. Kuhn, *Trans. Inst. Met. Finish.*, **71(2)**, 74 (1993).
22. M. Iwasaki, M. Hara and S. Ito, *J. Mater. Sci.*, **35**, 943 (2000).
23. V. Ravindran, R. M. Krishnan and V. S. Muralidharan, *Met. Finish.*, **96(11)**, 12 (1998).